


Please cite the Published Version

Akhmetkazyev, Yerassyl, Nauryzbayev, Galymzhan, Arzykulov, Sultangali, Rabie, Khaled  and Eltawil, Ahmed (2021) Ergodic capacity of cognitive satellite-terrestrial relay networks with practical limitations. In: International Conference on Information and Communication Technology Convergence (ICTC), 20 October 2021 - 22 October 2021, Jeju Island, Republic of Korea.

DOI: <https://doi.org/10.1109/ICTC52510.2021.9621131>

Publisher: IEEE

Version: Accepted Version

Downloaded from: <https://e-space.mmu.ac.uk/635050/>

Usage rights:  In Copyright

Additional Information: © 2021 IEEE. Personal use of this material is permitted. Permission from IEEE must be obtained for all other uses, in any current or future media, including reprinting/republishing this material for advertising or promotional purposes, creating new collective works, for resale or redistribution to servers or lists, or reuse of any copyrighted component of this work in other works.

Enquiries:

If you have questions about this document, contact openresearch@mmu.ac.uk. Please include the URL of the record in e-space. If you believe that your, or a third party's rights have been compromised through this document please see our Take Down policy (available from <https://www.mmu.ac.uk/library/using-the-library/policies-and-guidelines>)

Ergodic Capacity of Cognitive Satellite-Terrestrial Relay Networks with Practical Limitations

Yerassyl Akhmetkazyev, Galymzhan Nauryzbayev, [°]Sultangali Arzykulov, [§]Khaled Rabie, and [°]Ahmed Eltawil
School of Engineering and Digital Sciences, Nazarbayev University, Nur-Sultan, 010000, Kazakhstan
[°]Computer, Electrical, and Mathematical Sciences & Engineering Division, KAUST, Thuwal, KSA 23955-6900
[§]Department of Engineering, Manchester Metropolitan University, Manchester, M15 6BH, UK
Email: {yerassyl.akhmetkazyev, galymzhan.nauryzbayev}@nu.edu.kz,
[°]{sultangali.arzykulov@gmail.com, ahmed.eltawil@kaust.edu.sa}, [§]k.rabie@mmu.ac.uk

Abstract—This paper investigates the impact of practical limitations, such as transceiver hardware impairments and channel state information mismatch, on a cognitive hybrid satellite-terrestrial relay network. Moreover, it is assumed that the network is under the effect of independent and non-identically distributed interference noises emerging from neighboring device nodes. Generalized closed-form expressions of ergodic capacity for a terrestrial user are obtained considering the interference temperature constraint's influence. Finally, derived findings are validated through Monte Carlo simulation and the impact of impairments is examined.

Index Terms—Satellite-terrestrial relay network (STRN), cognitive radio (CR), interference temperature constraint (ITC), ergodic capacity (EC).

I. INTRODUCTION

SATELLITE communication has become a promising solution for providing future high capacity, ubiquitous connection services to terrestrial users in sparsely populated remote locations and emergency areas [1]. Moreover, satellite communication is noted as a viable facilitator of upcoming fifth-generation (5G) and beyond networks, which is believed to witness an enormous data traffic increase [2]. Therefore, this may lead to a serious problem as a spectrum shortage [3]. However, this issue can be overcome through using the cognitive radio (CR) method which allows primary and secondary users (SUs) to share the spectrum [4]. In [5], [6], the underlay CR were examined in satellite-terrestrial networks (STNs) aiming the more effective use of spectrum band. For example, the authors in [5] examined the coverage performance and failure probability of CR-based STN considering various practical limitations while outage performance was evaluated for a similar system model taking into account the interference temperature constraint (ITC) in [6].

One of the main challenges of the STN is the fact that shadowing and various type of barriers between the satellite transmitter and terrestrial receivers can lead to a masking effect, making line-of-sight (LoS) communication challenging to sustain in realistic satellite systems [7]. As a remedy, the cognitive hybrid satellite-terrestrial relay network (STRN), which incorporates relaying base stations to support satellite communication and boosts its stability and throughput, has been attracting significant interest both from business and academia recently [8]–[11]. For instance, the authors in [8], investigated

the system performance of integrated cognitive STRN in terms of ergodic capacity (EC). Furthermore, in [9], the authors considered both amplify-and-forward (AF) and decode-and-forward (DF) relaying techniques to investigate cooperative spectrum sharing schemes in satellite-terrestrial overlay networks. In addition, the performance of downlink hybrid STRN was examined in [10] by deriving an analytical expression of EC assuming AF scheme and taking into account co-channel interference. In [11], the authors evaluated the performance of CR-based STRN in terms of outage and EC, though not achieving closed-form EC expressions.

To the best of the authors' knowledge, most of the research works have not reported the impact of interference noises created by surrounding device nodes that are independent and non-identically distributed (i.n.i.d.) in the STRN model. Taking into account this fact and considering imperfect channel state information (CSI) and hardware impairment (HI) as well as ITC, the paper examines the performance of cognitive hybrid STRN in contrast to the aforementioned papers.

Hence, the main outcomes of the work are listed below. First, for the considered cognitive hybrid STRN, we derive analytical closed-form EC solutions for terrestrial users. Further, the impact of different practical restrictions is examined using the analytical findings and their accuracy is validated through Monte Carlo simulations. Finally, the deteriorative impact of i.n.i.d. interference nodes were demonstrated explicitly.

II. SYSTEM MODEL

We examine the downlink underlay cognitive hybrid STRN shown in Fig. 1, which includes primary and secondary networks (i.e., PN and SN). PN consists of primary transmitters, U_n , $n \in \mathcal{A} = \{1, 2, \dots, N\}$, and a primary receiver, K . At the same time, SN consists of a satellite transmitter, S , and a terrestrial relay, R , which is able to use the licensed spectrum of a primary receiver and communicate with SU, denoted by T . It is assumed that there is no direct communication from a satellite to terrestrial users due to the masking effect [7], [12]. Hence, R is utilized with a half-duplex DF protocol to support the communication. Hence, the primary transmitters can be treated as interference nodes to R and T .

A. Channel Models

We use a linear minimal mean square error channel estimator to represent the communication channels [13] as $\chi = \tilde{\chi} + \epsilon$, where χ and $\tilde{\chi}$ represent the measured and actual channel coefficients, respectively. ϵ denotes the error of measurement, with $\mathcal{CN}(0, \lambda)$ and $\lambda = \Phi\omega^{-\eta}$, where ω is the nominal transmit signal-to-noise ratio (SNR). If $\eta \rightarrow \infty$ for $\omega > 0$ then an ideal CSI can be obtained. Furthermore, with a mean of zero and variance σ^2 , additive white Gaussian noise (AWGN) subjects all receiving nodes.

1) *Satellite Link*: The channel corresponding to the satellite link given by h_{SR} is obeyed by shadowed-Rician fading. As a result, the probability density function (PDF) is as in [14]

$$f_{|\chi_s|^2}(x) = \sum_{\ell=0}^{m_s-1} \Upsilon x^\ell e^{-\partial_s x}, \quad x \geq 0, \quad (1)$$

where $\Upsilon = \frac{1}{2b_s} \left(\frac{2\bar{b}_s m_s}{2b_s m_s + \Omega_s} \right)^{m_s} \frac{(1-m_s)_\ell (-\delta_s)^\ell}{(\ell!)^2}$ and $\partial_s = \varrho_s - \delta_s$ with $\delta_s = \frac{\Omega_s}{2b_s(2b_s m_s + \Omega_s)}$ and $\varrho_s = \frac{1}{2b_s}$. Here, $2\bar{b}_s$ refers to the multi-path component's averaged power, while the line-of-sight (LoS) is characterized by the average power Ω_s . m_s indicates the severity of fading. Moreover, we define the satellite channels' path-loss as L which linearly depends on a logarithmic distance, as stated by Friis' law of free-space propagation [15].

Now, let us identify the satellite antenna gains, G_S . Our antenna array can be characterized by three parameters. The angle between the location of the relay and the beam core in relation to the satellite is represented by φ . Then, we can adopt the beam gain $G_i(\varphi)$ from [16] as $G_i(\varphi) = G_{i,\max} \left(\frac{J_1(u)}{2u} + 36 \frac{J_3(u)}{u^3} \right)^2$, where $J_l(\cdot)$ denotes the Bessel function of the 1st kind and l th order, and the second parameter, $u = 2.07 \frac{\sin \varphi}{\sin \varphi_{3\text{dB}}}$, and the third parameter, $\varphi_{3\text{dB}}$, represents the beam's constant 3-dB angle.

2) *Terrestrial Direct Channels*: The terrestrial direct channels, denoted by h_{RT} and h_{RK} , follow the Nakagami- m fading. Thus, the channel powers are Gamma random variables (RVs) with the PDF expressed as

$$f_{|\chi_n|^2}(z) = z^{m_z-1} e^{-\frac{z}{\nu_z}} / \Gamma(m_z) \nu_z^{m_z}, \quad (2)$$

where m_z and ν_z are the shape parameter and scale parameters.

Furthermore, analog beamforming between communicating nodes was modeled using the sectored antenna pattern, denoted by $G(\theta) = G_m$, if $\theta \leq \theta_b$; in all other cases, $G(\theta) = G_s$. Particularly, here G_m represents the main lobe gain while G_s indicates the side lobe gain. Here, within the context of specified main or side lobe sectors, an antenna gain is assumed to be constant. The angle of a boresight path is θ , and the antenna beamwidth is θ_b . For simplicity, it is presumed that the base station intrudes the PN users with side lobe gain, whereas the terrestrial direct links employ main lobe gain.

3) *Terrestrial Interference Channels*: Here, \mathbf{g}_{UR} and \mathbf{g}_{UT} represent the terrestrial interference channels and follow the Nakagami- m fading model. Now, let us consider $U_{n \in \mathcal{A}}$ are non-negative i.n.i.d. Gamma RVs with \tilde{m}_n and $\tilde{\nu}_n$ parameters.

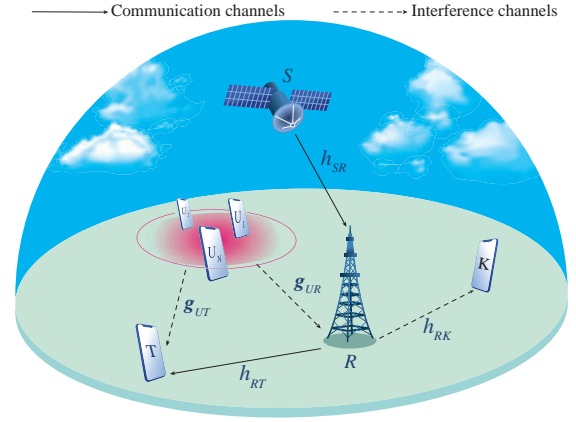


Fig. 1. Cognitive hybrid STRN model.

The PDF of $Q = \sum_{n=1}^N U_n$ is given as

$$f_Q(q) = q^{m_q-1} e^{-\frac{q}{\nu_q}} / \Gamma(m_q) \nu_q^{m_q}, \quad (3)$$

where an approximated scale parameter of a single Gamma function, ν_q , is evaluated by solving a set of equations $\frac{\mu}{2} - 2 \sum_{n=1}^N \frac{\tilde{m}_n \tilde{\nu}_n^3}{(\tilde{\nu}_n + \nu_q)^2} = 0$ and $\mu = \sum_{n=1}^N \tilde{m}_n \tilde{\nu}_n$. The corresponding shape parameter is evaluated as $m_q = \frac{\mu}{\nu_q}$.

B. Signal and SINR Models

The transmission of signal is implemented in two time slots. At first, S transmits the signal x to R with the transmission power of P_S . Thus, taking into account the aforementioned CSI mismatches, the received signal at R is expressed as

$$y_R = \left(\tilde{h}_{SR} + \epsilon_{SR} \right) \sqrt{P_S G_S G_R(\varphi) L} (x_R + \mu_{SR}) + \sum_{n=1}^N g_{UR_n} \sqrt{P_I G_s G_n d_{UR_n}^{-\tau}} (s_{UR_n} + \bar{\mu}_{UR_n}) + n_R, \quad (4)$$

with $n_R \sim \mathcal{CN}(0, \sigma_R^2)$ representing the AWGN. $\mu_{SR} \sim \mathcal{CN}(0, \kappa_{SR}^2)$ and $\bar{\mu}_{UR_n} \sim \mathcal{CN}(0, \bar{\kappa}_{UR_n}^2)$ reflect the influence of HIs, where κ_{SR} and $\bar{\kappa}_{UR_n}$ are the hardware imperfection levels in the transmitter-receiver pairs' communication channels.

Now, the signal-to-interference-noise-distortion ratio (SINDR) to decode message x_R can be written by arranging $a = P_S G_S G_R(\varphi) L$, $b = P_S G_S G_R(\varphi) L \kappa_{SR}$, $X = |\tilde{h}_{SR}|^2$, and $Q_{UR} = \sum_{n=1}^N U_{UR_n}$, where $U_{UR_n} = g_{UR_n} (1 + \bar{\kappa}_{UR_n}^2) P_I G_s G_n d_{UR_n}^{-\tau}$ as follows

$$\gamma_R = aX / (bX + \Sigma_R + Q_{UR}), \quad (5)$$

where $\Sigma_R = a(1 + \kappa_{SR}^2) \sigma_\epsilon^2 + \sigma_R^2$ denotes the channel error power and AWGN.

In the second time slot, the signal is forwarded further to T with the aid of a DF protocol. Therefore, the received signal at T can be obtained as

$$r_T = \left(\tilde{h}_{RT} + \epsilon_{RT} \right) \sqrt{P_R G_R G_m d_{RT}^{-\tau}} (x_T + \mu_{RT})$$

$$+ g_{UT_n} \sum_{n=1}^N \sqrt{P_I G_s G_n d_{UT_n}^{-\tau}} (s_{UT_n} + \bar{\mu}_n) + w_T. \quad (6)$$

Finally, the respective SINDR to decode x_T can be written as

$$\psi_T = \frac{W_1 Z P_R}{P_R (W_2 Z + E) + Q_{UT} + \sigma_T^2}, \quad (7)$$

where the following denotations are introduced: $W_1 = G_R G_m d_{RT}^{-\tau}$, $W_2 = G_R G_m d_{RT}^{-\tau} \kappa_{RT}$ and $Z = |\tilde{h}_{RT}|^2$, $Q_{UT} = \sum_{n=1}^N U_{UT_n}$ with $U_{UT_n} = g_{UT_n} (1 + \bar{\kappa}_{UT_n}^2) P_I G_s G_n d_{UT_n}^{-\tau}$ and $E = G_R G_m d_{RT}^{-\tau} (1 + \kappa_{RT}^2) \sigma_\epsilon^2$.

III. ERGODIC CAPACITY

We dedicate this section to derive an exact closed-form solution for the EC under practical conditions such as hardware distortion, interference noises, and imperfect CSI scenarios. We define the system's effective EC as the minimum of two hops

$$EC = \min(EC_{SR}, EC_{RT}), \quad (8)$$

where EC_{SR} and EC_{RT} denote the ECs related to the S -to- R and R -to- T links, respectively.

A. Derivation of EC_{SR}

Thus, using Eq. (5), the EC_{SR} can be given by definition as

$$EC_{SR} = \mathbb{E} \{\log_2(1 + \gamma_R)\} \quad (9)$$

By using Eq. (5) and the property of a logarithm function, Eq. (9) can be further written as a difference of two terms

$$EC_{SR} = \mathbb{E} \{\log_2(X(a+b) + Q_{UR} + \Sigma_R)\} - \mathbb{E} \{\log_2(Xb + Q_{UR} + \Sigma_R)\}. \quad (10)$$

To make it concise the following denotations were introduced: $J = X(a+b) + Q_{UR}$ and $H = Xb + Q_{UR}$. Hence, the simplified representation for the ergodic capacity can be obtained as

$$EC_{SR} = \underbrace{\mathbb{E} \{\log_2(J + \Sigma_R)\}}_{C_1} - \underbrace{\mathbb{E} \{\log_2(H + \Sigma_R)\}}_{C_2}. \quad (11)$$

Proposition 1: Considering imperfect CSI and HI as well as i.n.i.d. interfering nodes, the closed-form expressions of C_1 and C_2 for EC_{SR} can be expressed as

$$C_1 = \sum_{\ell=0}^{m_s-1} \Upsilon \sum_{i=0}^{m_q-1} \binom{m_q-1}{i} \frac{(-a+b)^i \partial_s^{-i-\ell-1}}{\ln(2)\Gamma(m_q)\nu_q^i} \times G_{1,1}^{1,1} \left(-\frac{a+b}{\nu_q \partial_s} \Big|_0^{-i-\ell} \right) G_{3,2}^{1,3} \left(\frac{\nu_q}{\Sigma_R} \Big|_{1,0}^{i-m_q+1,1,1} \right), \quad (12)$$

$$C_2 = \sum_{\ell=0}^{m_s-1} \Upsilon \sum_{i=0}^{m_q-1} \binom{m_q-1}{i} \frac{(-b)^i \partial_s^{-i-\ell-1}}{\ln(2)\Gamma(m_q)\nu_q^i} \times G_{1,1}^{1,1} \left(-\frac{b}{\nu_q \partial_s} \Big|_0^{-i-\ell} \right) G_{3,2}^{1,3} \left(\frac{\nu_q}{\Sigma_R} \Big|_{1,0}^{i-m_q+1,1,1} \right). \quad (13)$$

Proof: The details are shown in Appendix A. ■

Remark Please note that the above closed-form expression is true while $\frac{a+b}{\nu_q} \leq \partial_s$ and $\frac{b}{\nu_q} \leq \partial_s$, respectively.

B. Derivation of EC_{RT}

Now the EC_{RT} can be derived taking into account ITC and using Eq. (7) as

$$EC_{RT} = \underbrace{\Pr\{P_R \leq S\}}_{P_1} \underbrace{\mathbb{E}\{\log_2(1 + K_1)\}}_{M_1} + \underbrace{\Pr\{P_R > S\}}_{P_2} \underbrace{\mathbb{E}\{\log_2(1 + K_2)\}}_{M_2}, \quad (14)$$

where $K_1 = \frac{W_1 Z P_R}{P_R (W_2 Z + E) + Q_{UT} + \sigma_T^2}$ and $K_2 = \frac{W_1 Z S}{S(W_2 Z + E) + Q_{UT} + \sigma_T^2}$. $S = \frac{I_{ITC}^*}{Y}$ and $P_R = \min(\bar{P}_R, S)$. Further, let us denote $I_{ITC}^* = I_{ITC} d_{RK}^{\tau}$, $Y = |h_{RK}|^2$ and $\Lambda = \frac{ITC^*}{P_R}$.

Proposition 2: EC_{RT} , expressed by Eq. (14), is solved in closed-form with the aid of $P_1 = \frac{\gamma(m_y, \frac{\Lambda}{\nu_y})}{\Gamma(m_y)}$, $P_2 = \frac{\Gamma(m_y, \frac{\Lambda}{\nu_y})}{\Gamma(m_y)}$ and M_1, M_2 terms as in Eqs. (15) and (16), where, for the sake of brevity, the terms are demonstrated separately.

$$M_1 = G_{3,2}^{1,3} \left(\frac{\hat{\nu}_j}{P_R E + \sigma_T^2} \Big|_{1,0}^{1-\hat{m}_j,1,1} \right) / \ln(2)\Gamma(\hat{m}_j) - G_{3,2}^{1,3} \left(\frac{\hat{\nu}_h}{P_R E + \sigma_T^2} \Big|_{1,0}^{1-\hat{m}_h,1,1} \right) / \ln(2)\Gamma(\hat{m}_h). \quad (15)$$

Proof: The detailed solution is shown in Appendix B. ■

C. Interference-free EC

Here, we consider the interference-free scenario (i.e., $Q_{UR} = Q_{UT} = 0$). The corresponding closed-form expression for EC_{SR}^{IF} can be derived as

$$EC_{SR}^{IF} = \sum_{\ell=0}^{m_s-1} \Upsilon \frac{\partial_s^{-\ell-1}}{\ln(2)} \left(G_{3,2}^{1,3} \left(\frac{a+b}{\Sigma_R \partial_s} \Big|_{1,0}^{-\ell,1,1} \right) - G_{3,2}^{1,3} \left(\frac{b}{\Sigma_R \partial_s} \Big|_{1,0}^{-\ell,1,1} \right) \right), \quad (17)$$

and the M_1^{IF} and M_2^{IF} terms of EC_{RT}^{IF} can be obtained as in Eqs. (18) and (19).

$$M_1^{IF} = G_{3,2}^{1,3} \left(\frac{\hat{\nu}_j^{IF}}{P_R E + \sigma_T^2} \Big|_{1,0}^{1-\hat{m}_j^{IF},1,1} \right) / \ln(2)\Gamma(\hat{m}_j^{IF}) - G_{3,2}^{1,3} \left(\frac{\hat{\nu}_h^{IF}}{P_R E + \sigma_T^2} \Big|_{1,0}^{1-\hat{m}_h^{IF},1,1} \right) / \ln(2)\Gamma(\hat{m}_h^{IF}). \quad (18)$$

IV. NUMERICAL RESULTS

This section presents numerical results on the ergodic capacity of the network scheme considered in the paper, as specified by the parameters shown in Table I. Monte Carlo simulations are also used to verify derived mathematical findings. One can notice that there is some gap between analytical and simulation

$$M_2 = \log_2 \left(I_{\text{ITC}}^* (W_1 + W_2) \frac{(m_z + m_y - 1)! \Gamma(m_z + 1) \Gamma(m_y - 1)}{\Gamma(m_z) \Gamma(m_y)} \frac{\nu_z}{\nu_y} + EI_{\text{ITC}}^* \frac{\Gamma(m_y - 1)}{\Gamma(m_y) \nu_y} + \frac{m_q! \nu_q}{\Gamma(m_q)} + \sigma_T^2 \right) - \log_2 \left(I_{\text{ITC}}^* W_2 \frac{(m_z + m_y - 1)! \Gamma(m_z + 1) \Gamma(m_y - 1)}{\Gamma(m_z) \Gamma(m_y)} \frac{\nu_z}{\nu_y} + EI_{\text{ITC}}^* \frac{\Gamma(m_y - 1)}{\Gamma(m_y) \nu_y} + \frac{m_q! \nu_q}{\Gamma(m_q)} + \sigma_T^2 \right) \quad (16)$$

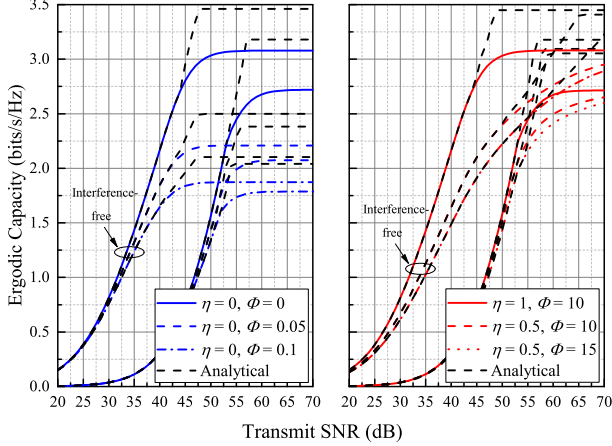


Fig. 2. The EC vs. the transmit SNR for different CSI scenarios.

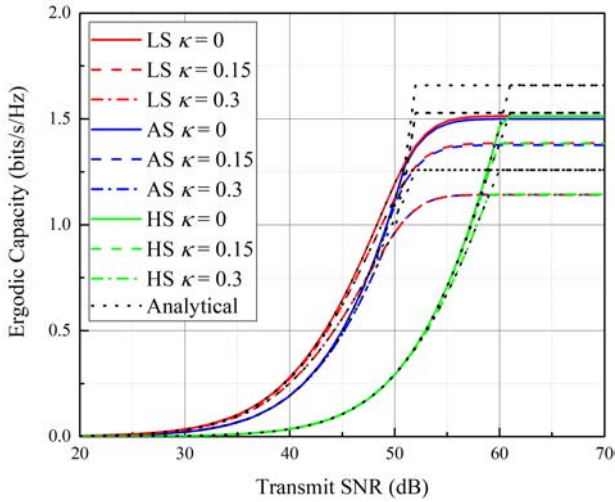


Fig. 3. EC with various HI levels for different shadowing cases.

plots after the pre-determined ITC level. This can be explained by the fact that M_2 in Eq. (14) was obtained as its upper bound while the rest of our analytical findings represent exact EC and agree with Monte Carlo simulation.

In Fig. 2, the perfect CSI case and influence of the CSI mismatch are demonstrated. It also takes into account SNR-independent and SNR-dependent CSI scenarios. Particularly, the channel error variance is said to be free from the transmit SNR if $\eta = 0$, and in that case Φ is found to have a substantial impact on system performance. Interestingly, at low SNR values, Φ has no impact on system performance influencing distinctively only starting at 50 dB. It occurs because the CSI

Table I. Simulation parameters.

Parameter	Value
Terrestrial antenna gains, $\{G_m, G_s\}$	$\{12, -1.1092\}$ dB
Terrestrial channel parameter, m	2
Satellite antenna gains, $\{G_T, G_{i,max}\}$	$\{4.8, 54\}$ dB
Satellite channel parameters, $\{m_s, b_s, \Omega_s\}$	$\{5, 0.251, 0.279\}$
Path-loss exponent, τ	2
Orbit height, D	35786 km
Interference noise power	25 dB
R -to- T distance, d_{RT}	100 m
R -to- K distance, d_{RK}	50 m
3dB angle, φ_{3dB}	0.4°
Temperature, T	300 K
Carrier frequency, f_c	2 GHz
Carrier bandwidth, \mathcal{W}	15 MHz

strives to be ideal as Φ approaches zero. As a result, for low SNR values, a marginal CSI mismatch has a little effect on the performance. On the other hand, CSI is said to be SNR-dependent and maintain saturation only at larger SNR rates than the SNR-independent CSI if it is set as $\eta \neq 0$. The rise in η leads to a boost in system performance, as can be seen. However, in the situation with equivalent η values, increasing Φ provokes a minor deterioration in system performance. It's worth noting that η has a far greater impact on results than Φ . In addition, Fig. 2 demonstrates the same investigation for the interference-free case. It can be seen that the system performance becomes superior in the absence of interference. Furthermore, one can easily notice that CSI mismatches have a greater impact for the interference-free scenario.

Fig. 3 investigates the impact of hardware imperfections under the various shadowing scenarios for the satellite links. The HI amount was specifically configured to three separate cases with $\kappa = \{0, 0.15, 0.3\}$. Moreover, heavy, average and light shadowed-Rician fading models are considered with parameters (m_s, b_s, Ω_s) as $(2, 0.063, 0.0005)$, $(5, 0.251, 0.279)$, and $(10, 0.158, 1.29)$, respectively. In the presence of HI, system performance degrades noticeably, as predicted. It is worth noting that HIs have a minor effect at low SNRs. However, it is clear that a greater value of HI, i.e., $\kappa = 0.3$, significantly degrades the overall system performance in terms of EC. One can notice from the plot that the light shadowed-Rician fading allows us to obtain the best EC rate at a lower transmit SNR while heavy shadowing results in the worst system performance, as expected.

Fig. 4 illustrates the EC versus the number of the interference nodes for the different levels of the transmit SNR, i.e. $\{40, 50, 60\}$ dB. It can be clearly seen that system performance deteriorates with the increasing number of interference nodes as expected. Moreover, one can notice that a higher level of

$$M_2^{IF} = \log_2 \left(I_{\text{ITC}}^* (W_1 + W_2) \frac{(m_z + m_y - 1)! \Gamma(m_z + 1) \Gamma(m_y - 1)}{\Gamma(m_z) \Gamma(m_y)} \frac{\nu_z}{\Gamma(m_z + m_y)} \nu_y + E I_{\text{ITC}}^* \frac{\Gamma(m_y - 1)}{\Gamma(m_y) \nu_y} + \sigma_T^2 \right) - \log_2 \left(I_{\text{ITC}}^* W_2 \frac{(m_z + m_y - 1)! \Gamma(m_z + 1) \Gamma(m_y - 1)}{\Gamma(m_z) \Gamma(m_y)} \frac{\nu_z}{\Gamma(m_z + m_y)} \nu_y + E I_{\text{ITC}}^* \frac{\Gamma(m_y - 1)}{\Gamma(m_y) \nu_y} + \sigma_T^2 \right) \quad (19)$$

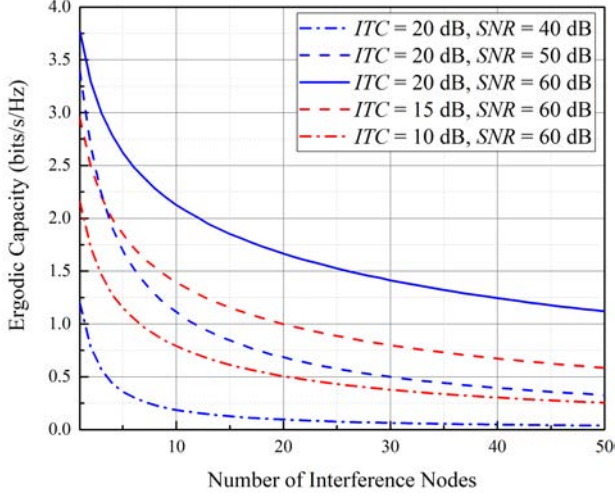


Fig. 4. EC vs. number of interference nodes for different ITC.

the transmit SNR ensures a better performance. Moreover, the impact of various ITC levels, i.e., {10, 15, 20} dB, is also investigated in the graph. It can be seen that a lower level of ITC leads to system performance degradation in terms of EC by limiting the access to the primary user's spectrum band.

V. CONCLUSION

In this paper, the performance of cognitive hybrid satellite-terrestrial relay network was examined where terrestrial SU enjoys access to the spectrum of PUs limited only by ITC. Moreover, we obtained closed-form EC expressions taking into consideration the practical limitations such as SNR-dependent/independent CSI, hardware impairments as well as i.n.i.d. interference noises. Furthermore, simulation results demonstrated the deteriorative impact of each system model imperfections in detail. Particularly, it was shown that the number of interfering nodes has a significant effect on the system performance hence cannot be neglected. Finally, Monte Carlo simulations verified the derived analytical results.

APPENDIX A ERGODIC CAPACITY EC_{SR}

Here, the derivation steps for the EC_{SR} are presented, particularly Eq. (11) can be further expanded as

$$EC_{SR} = \mathbb{E} \left\{ \log_2 \left(\Sigma_R \left(1 + \frac{J}{\Sigma_R} \right) \right) \right\} - \mathbb{E} \left\{ \log_2 \left(\Sigma_R \left(1 + \frac{H}{\Sigma_R} \right) \right) \right\}$$

$$= \underbrace{\int_0^\infty \log_2 \left(1 + \frac{j}{\Sigma_R} \right) f_J(j) dj}_{C_1} - \underbrace{\int_0^\infty \log_2 \left(1 + \frac{h}{\Sigma_R} \right) f_H(h) dh}_{C_2}. \quad (20)$$

Now, let us first define $f_J(j)$ and $f_H(h)$. Since J is the summation of two RVs, its PDF can be defined as

$$f_J(j) = \int_0^\infty f_X(x) f_Q(q) dx dq = \int_0^\infty f_Q(j - (a+b)x) f_X(x) dx. \quad (21)$$

Here, Q is approximated as (3), and X follows shadowed Rician fading, thus

$$f_J(j) = \int_0^\infty \frac{(j - (a+b)x)^{m_q-1}}{\Gamma(m_q) \nu_q^{m_q} e^{\frac{j-(a+b)x}{\nu_q}}} \sum_{\ell=0}^{m_s-1} \Upsilon x^\ell e^{-\partial_s x} dx = \frac{e^{-\frac{j}{\nu_q}}}{\Gamma(m_q) \nu_q^{m_q}} \sum_{\ell=0}^{m_s-1} \Upsilon \sum_{i=0}^{m_q-1} \binom{m_q-1}{i} j^{m_q-1-i} \times (- (a+b))^\ell \partial_s^{-i-\ell-1} G_{1,1}^{1,1} \left(-\frac{a+b}{\nu_q \partial_s} \middle|_{-i-\ell} \right). \quad (22)$$

In the same manner, $f_H(h)$ can be obtained. Next, $\mathbb{E} \left\{ \ln \left(1 + \frac{j}{\Sigma_R} \right) \right\}$ can be re-written by using [18, Eq. (8.4.6.5)], with the aid of a Meijer G-function as $\ln \left(1 + \frac{j}{\Sigma_R} \right) = G_{2,2}^{1,2} \left(\frac{j}{\Sigma_R} \middle|_{1,1} \right)$. Then, C_1 and C_2 are evaluated using [19, Eq. (7.813.1)] as in Eqs. (12) and (13).

APPENDIX B ERGODIC CAPACITY EC_{RT}

In this section the derivation steps of EC_{RT} are demonstrated. First, by using the property of a logarithm function, let us rewrite M_1 as a difference of two terms as

$$M_1 = \mathbb{E} \left\{ \log_2 (Z(W_1 P_R + W_2 P_R) + Q_{UT} + P_R E + \sigma_T^2) \right\} - \mathbb{E} \left\{ \log_2 (P_R W_2 Z + P_R E + Q_{UT} + \sigma_T^2) \right\}. \quad (23)$$

Further, to make it concise let us introduce the following denotations: $J = Z(W_1 P_R + W_2 P_R) + Q_{UT}$ and $H = P_R W_2 Z + Q_{UT}$. Now, the closed-form expression for M_1 can be evaluated as follows

$$M_1 = \mathbb{E} \left\{ \log_2 (J + P_R E + \sigma_T^2) \right\} - \mathbb{E} \left\{ \log_2 (H + P_R E + \sigma_T^2) \right\}$$

$$\begin{aligned}
&= \underbrace{\int_0^\infty \log_2 \left(1 + \frac{j}{P_R E + \sigma_T^2} \right) f_J(j) \, dj}_{M_{11}} \\
&\quad - \underbrace{\int_0^\infty \log_2 \left(1 + \frac{h}{P_R E + \sigma_T^2} \right) f_H(h) \, dh}_{M_{12}}. \quad (24)
\end{aligned}$$

Let us first define $f_J(j)$ and $f_H(h)$. Since both J and H are the summations of two RVs, we can define them using Gamma representation $J \sim \text{Gamma}(\hat{m}_j, \hat{\nu}_j)$ and $H \sim \text{Gamma}(\hat{m}_h, \hat{\nu}_h)$, respectively. Then, M_{11} and M_{12} are evaluated as

$$\begin{aligned}
M_{11} &= \int_0^\infty \frac{j^{\hat{m}_j-1} e^{-\frac{j}{\hat{\nu}_j}}}{\ln(2)\Gamma(\hat{m}_j)\hat{\nu}_j^{\hat{m}_j}} G_{2,2}^{1,2} \left(\frac{j}{P_R E + \sigma_T^2} \middle|_{1,0}^{1,1} \right) dj \\
&= G_{3,2}^{1,3} \left(\frac{\hat{\nu}_j}{P_R E + \sigma_T^2} \middle|_{1,0}^{1-\hat{m}_j,1,1} \right) / \ln(2)\Gamma(\hat{m}_j), \quad (25)
\end{aligned}$$

$$\begin{aligned}
M_{12} &= \int_0^\infty \frac{h^{\hat{m}_h-1} e^{-\frac{h}{\hat{\nu}_h}}}{\ln(2)\Gamma(\hat{m}_h)\hat{\nu}_h^{\hat{m}_h}} G_{2,2}^{1,2} \left(\frac{h}{P_R E + \sigma_T^2} \middle|_{1,0}^{1,1} \right) dh \\
&= G_{3,2}^{1,3} \left(\frac{\hat{\nu}_h}{P_R E + \sigma_T^2} \middle|_{1,0}^{1-\hat{m}_h,1,1} \right) / \ln(2)\Gamma(\hat{m}_h). \quad (26)
\end{aligned}$$

Now, M_2 can be solved only in upper bound due to its complexity (i.e., there are three RVs), therefore, let us transform M_2 from the exact form to the upper bound expression as

$$\begin{aligned}
M_2 &= \mathbb{E} \left\{ \log_2 \left(\frac{I_{\text{ITC}}^*}{Y} (Z(W_1 + W_2) + E) + Q_{UT} + \sigma_T^2 \right) \right\} \\
&\quad - \mathbb{E} \left\{ \log_2 \left(\frac{Z I_{\text{ITC}}^* W_2}{Y} + \frac{E I_{\text{ITC}}^*}{Y} + Q_{UT} + \sigma_T^2 \right) \right\} \\
&= \log_2 \left(\underbrace{\mathbb{E} \left\{ \frac{Z I_{\text{ITC}}^* (W_1 + W_2)}{Y} \right\}}_{M_{21}} + M_{22} + M_{23} + \sigma_T^2 \right) \\
&\quad - \log_2 \left(\underbrace{\mathbb{E} \left\{ \frac{Z I_{\text{ITC}}^* W_2}{Y} \right\}}_{M_{24}} + M_{22} + M_{23} + \sigma_T^2 \right), \quad (27)
\end{aligned}$$

where $M_{22} = \mathbb{E} \left\{ \frac{E I_{\text{ITC}}^*}{Y} \right\}$ and $M_{23} = \mathbb{E} \{Q_{UT}\}$. By taking

$\Psi = \frac{Z}{Y}$ and estimating its corresponding PDF as $f_\Psi(\psi) = \frac{\psi^{m_z-1} (m_z+m_y-1)!}{\Gamma(m_z)\nu_z^{m_z}\Gamma(m_y)\nu_y^{m_y}} \left(\frac{1}{\nu_y}\right)^{-m_z-m_y} \left(1 + \frac{\psi\nu_y}{\nu_z}\right)^{-m_z-m_y}$ and the fact that $(1 + c\gamma)^{-d} = \frac{1}{\Gamma(d)} G_{1,1}^{1,1}(c\gamma|_0^{1-d})$ [20, Eq. (7.34.3.46.1)], M_{21} , M_{22} , M_{23} can be obtained as follows

$$\begin{aligned}
M_{21} &= I_{\text{ITC}}^* (W_1 + W_2) \frac{(m_z + m_y - 1)!}{\Gamma(m_z)\Gamma(m_y)} \\
&\quad \times \frac{\Gamma(m_z + 1)\Gamma(m_y - 1)}{\Gamma(m_z + m_y)} \frac{\nu_z}{\nu_y}. \quad (28)
\end{aligned}$$

$$M_{22} = E I_{\text{ITC}}^* \int_0^\infty y \frac{y^{-m_y-1} e^{-\frac{1}{y\nu_y}}}{\Gamma(m_y)\nu_y^{m_y}} dy$$

$$= E I_{\text{ITC}}^* \frac{\Gamma(m_y - 1)}{\Gamma(m_y)\nu_y}. \quad (29)$$

$$M_{23} = \int_0^\infty q \frac{q^{m_q-1} e^{-\frac{q}{\nu_q}}}{\Gamma(m_q)\nu_q^{m_q}} dq = \frac{m_q! \nu_q}{\Gamma(m_q)}. \quad (30)$$

In the same manner, M_{24} can be calculated, and finally M_2 can be derived as Eq. (16).

REFERENCES

- [1] Q. Huang *et al.*, "Energy Efficient Beamforming Schemes for Satellite-Aerial-Terrestrial Networks," *IEEE Trans. Commun.*, vol. 68, no. 6, pp. 3863-3875, June 2020.
- [2] L. Dai *et al.*, "A Survey of Non-Orthogonal Multiple Access for 5G," *IEEE Commun. Surv. Tutor.*, vol. 20, no. 3, pp. 2294-2323, 3rd quarter 2018.
- [3] G. Giambene, S. Kota and P. Pillai, "Satellite-5G Integration: A Network Perspective," *IEEE Netw.*, vol. 32, no. 5, pp. 25-31, Oct. 2018.
- [4] Y. Ruan *et al.*, "Spectral-Energy Efficiency Tradeoff in Cognitive Satellite-Vehicular Networks Towards Beyond 5G," *IEEE Wireless Commun. Netw. Conf. (WCNC)*, Marrakesh, Morocco, pp. 1-6, 2019.
- [5] Y. Akhmetkazyev *et al.*, "Performance of NOMA-Enabled Cognitive Satellite-Terrestrial Networks With Non-Ideal System Limitations," *IEEE Access*, vol. 9, pp. 35932-35946, 2021.
- [6] Y. Akhmetkazyev *et al.*, "Cognitive Non-ideal NOMA Satellite-Terrestrial Networks with Channel and Hardware Imperfections," *IEEE Wireless Commun. Netw. Conf. (WCNC)*, 2021, pp. 1-6.
- [7] Q. Huang *et al.*, "Performance Analysis of Integrated Satellite-Terrestrial Multiantenna Relay Networks With Multiuser Scheduling," *IEEE Trans. Aerosp. Electron. Syst.*, vol. 56, no. 4, pp. 2718-2731, Aug. 2020.
- [8] R. Liu *et al.*, "Performance Evaluation of NOMA-Based Cognitive Integrated Satellite Terrestrial Relay Networks With Primary Interference," *IEEE Access*, vol. 9, pp. 71422-71434, 2021.
- [9] X. Zhang *et al.*, "Vickrey Auction-Based Secondary Relay Selection in Cognitive Hybrid Satellite-Terrestrial Overlay Networks With Non-Orthogonal Multiple Access," *IEEE Wireless Commun. Lett.*, vol. 9, no. 5, pp. 628-632, May 2020.
- [10] V. Bankey and P. K. Upadhyay, "Ergodic Capacity of Multiuser Hybrid Satellite-Terrestrial Fixed-Gain AF Relay Networks With CCI and Outdated CSI," *IEEE Trans. Veh. Technol.*, vol. 67, no. 5, pp. 4666-4671, May 2018.
- [11] Anh-Tu Le *et al.*, "Enabling NOMA in Overlay Spectrum Sharing in Hybrid Satellite-Terrestrial Systems," *IEEE Access*, vol. 9, pp. 56616-56629, 2021.
- [12] K. An *et al.*, "Performance Analysis of Multi-Antenna Hybrid Satellite-Terrestrial Relay Networks in the Presence of Interference," *IEEE Trans. Commun.*, vol. 63, no. 11, pp. 4390-4404, Nov. 2015.
- [13] Y. Gao *et al.*, "Analysis of the Dynamic Ordered Decoding for Uplink NOMA Systems With Imperfect CSI," *IEEE Trans. Veh. Technol.*, vol. 67, no. 7, pp. 6647-6651, Jul. 2018.
- [14] A. Abdi *et al.*, "A new simple model for land mobile satellite channels: first- and second-order statistics," *IEEE Trans. Wireless Commun.*, vol. 2, no. 3, pp. 519-528, May 2003.
- [15] K. Guo *et al.*, "Outage analysis of cognitive hybrid satellite-terrestrial networks with hardware impairments and multi-primary users," *IEEE Wireless Commun. Lett.*, vol. 7, no. 5, pp. 816-819, Oct. 2018.
- [16] P. K. Sharma, D. Deepthi and D. I. Kim, "Outage Probability of 3-D Mobile UAV Relaying for Hybrid Satellite-Terrestrial Networks," *IEEE Commun. Lett.*, vol. 24, no. 2, pp. 418-422, Feb. 2020.
- [17] G. Naurzybayev, M. Abdallah, and K. M. Rabie, "Outage Probability of the EH-Based Full-Duplex AF and DF Relaying Systems in $\alpha - \mu$ Environment," *IEEE Veh. Technol. Conf. (VTC-Fall)*, Chicago, IL, USA, 2018, pp. 1-6.
- [18] A. P. Prudnikov, Y. A. Brychkov, and O. I. Marichev, *Integrals and Series, Volume 3: More Special Functions*. New York: Gordon and Breach, 1990.
- [19] I. S. Gradshteyn and I. M. Ryzhik, *Table of integrals, series, and products*. Elsevier/Academic Press, Amsterdam, 7th ed., 2007.
- [20] Wolfram, "The wolfram functions site." Last visited on 03/10/2020.